eCELLS & MATERIALS

OPEN ACCESS

CHARACTERIZATION OF TEMPOROMANDIBULAR JOINT ARTICULAR DISC PROGENITOR CELL CLONES

K.J. Weekes[1], P. Lam[1], C. Kim[1,2] and B. Johnstone[1,*]

[1] Department of Orthopaedics and Rehabilitation, Oregon Health & Science University, Portland, OR, USA
[2] College of Osteopathic Medicine of the Pacific Northwest, Western Health Science University, Lebanon, OR, USA

Abstract

A critical component of the temporomandibular joint (TMJ) is the fibrocartilage articular disc (AD). Researchers have attempted to regenerate the AD to alleviate TMJ osteoarthritis but alternative cell sources for use in AD regenerative approaches are needed due to insufficient extracellular matrix (ECM) production by total articular disc cells (TACs). Tissue-specific progenitor cells have been identified in many tissues. The aim of the present study was to identify adult multipotent progenitor cells within the AD suitable for regenerative medicine applications.

A novel AD progenitor cell population was identified in rhesus macaques. Clonally derived articular disc progenitor cells (ADPs) were isolated using fibronectin differential cell adhesion. ADPs represent between 1 and 3 % of the TAC population and are capable of *in vitro* expansion beyond 60 population doublings. ADPs were characterized using osteogenic, adipogenic, and fibrochondrogenesis differentiation assays. Clones exhibited phenotypic plasticity, differentiating into osteocytes, adipocytes, and fibrochondrocytes.

ECM secretion profiles following fibrochondrogenic differentiation were assessed using immunohistochemistry (IHC), fluorescently activated cell sorting (FACS), total collagen, and glycosaminoglycan (GAG) assays and compared with TACs, articular cartilage progenitor cells (ACPs), tendon progenitor cells (TPCs) and bone-marrow-derived mesenchymal stem cells (BMMSCs). ADP pellet cultures produced a biochemical phenotype similar to native AD tissue, with production of versican (VCAN) and collagen types I, II, III, and VI (COL1, COL2, COL3, COL6). However, clonally derived ADP cell lines produced different amounts of ECM and exhibited different expansion potentials. These findings indicated flexibility in clone selection for potential regenerative strategies to recapitulate native anisotropy.

Keywords: Cell biology, cell differentiation, temporomandibular joint (TMJ), temporomandibular disorders (TMDs), tissue engineering, stem cell(s), regenerative medicine.

***Address for correspondence**: Brian Johnstone PhD, Department of Orthopaedics and Rehabilitation, Oregon Health & Science University, 3181 SW Sam Jackson Park Rd., Mail Code: OP31, Portland, OR, 97239, USA. Telephone number: +1 5034949505 Email: johnstob@ohsu.edu

List of Abbreviations

ACP	articular cartilage progenitor cell
AD	articular disc
ADP	articular disc progenitor cell
APC	allophycocyanin
BGLAP	bone gamma carboxyglutamic acid-containing protein
BMMSC	bone-marrow-derived mesenchymal stem cell
BSA	bovine serum albumin
BV421	BD Horizon™ Brilliant Violet™ 421
CD	cluster of differentiation
CFE	colony-forming efficiency
COL1	collagen type I
COL1A1	collagen type I alpha 1 chain
COL2	collagen type II
COL2A1	collagen type II alpha 1 chain
COL3	collagen type III
COL3A1	collagen type III alpha 1 chain
COL6	collagen type VI
COL6A3	collagen type VI alpha 3 chain
Cy7	C7-cyanine
DAPI	4′,6-diamidino-2-phenylindole
DMEM/F12	Dulbecco's modified Eagle's medium/Ham's F12
DMMB	1,9-dimethymethylene blue
DTT	dithiothreitol

ECM	extracellular matrix
FABP4	fatty acid binding protein 4
FACS	fluorescently activated cell sorting
FBS	fetal bovine serum
FGF-2	fibroblast growth factor-2
FITC	fluorescein isothiocyanate
GAG	glycosaminoglycan
HEPES	4-(2-hydroxyethyl)-1-piperazineethanesulfonic acid
IHC	immunohistochemistry
PBS	phosphate-buffered solution
PE	phycoerythrin
PPARG	peroxisome proliferator-activated receptor gamma
qPCR	quantitative polymerase chain reaction
RNA	ribonucleic acid
RUNX2	Runt-related transcription factor 2
SOX9	SRY-related HMG-box 9
TAC	total articular disc cell population
TGF-β1	transforming growth factor-β1
TMJ	temporomandibular joint
TPC	tendon progenitor cell
VCAN	versican

Introduction

The TMJ is the most active joint in the human body; consequently, TMJ disorders are severely debilitating and a significant public health issue (Schiffman *et al.*, 2014). A component of the TMJ is the AD, which serves to attenuate forces generated between the mandibular condyle and the temporal bone during mastication (Fig. 1). The AD is composed of fibrocartilage containing COL1, with a minor quantity of COL2 (Detamore *et al.*, 2006; Murphy *et al.*, 2013; Tong and Tideman, 2001). Severe damage or disease associated with the AD may lead to surgical removal to restore some function to the joint. However, discectomies can lead to osteoarthritis and increased likelihood of jaw locking, hence the considerable interest in regeneration of TMJ ADs (Salash *et al.*, 2016).

Current methods for tissue engineering the TMJ AD are based on studies of hyaline cartilage and meniscus, which has led to an improved understanding of important mechanical and biochemical cues for *in vitro* development of these tissues (Mehrotra, 2013; Naujoks *et al.*, 2008). However, cells isolated from the TMJ do not produce as much ECM as other cell types, excluding them as an ideal cell source. The insufficient matrix production from TACs has stimulated a search for alternative cell types (Johns *et al.*, 2008).

Fibronectin panning was demonstrated to be an effective method to isolate adult tissue-specific progenitor cells from epidermal tissue, hyaline cartilage, and tendon (Dowthwaite *et al.*, 2004; Jones and Watt, 1993; Williams *et al.*, 2010; Williamson *et al.*, 2015). These progenitor cells are defined as having higher levels of fibronectin-binding cell surface integrin proteins, with progenitor attributes including self-renewal (clonal proliferation from single cells) and phenotypic plasticity within mesenchymal lineages (Jones and Watt, 1993; Williams *et al.*, 2010; Williamson *et al.*, 2015). Furthermore, comparisons of hyaline cartilage progenitors with BMMSCs indicate that the former are more restricted to differentiating into stable cartilage (Anderson *et al.*, 2016). Therefore, the strategy of the present study was to isolate tissue-specific progenitor cells with lineage restriction favoring AD fibrocartilage ECM production to recapitulate the AD structure.

In the present study, fibronectin panning was used to isolate novel ADPs from the TMJ of rhesus macaques, which is structurally and biochemically similar to the human TMJ (Kalpakci *et al.*, 2010). The study investigated whether ADPs possessed stem-cell-like properties and were capable of clonal expansion and phenotypic plasticity within the osteogenic, adipogenic, and chondrogenic lineages. Additionally, native rhesus macaque AD tissue was evaluated as a comparator for ADP ECM production, advancing the understanding of this species as a model for future clinical and regenerative medicine investigations.

Materials and Methods

Cell isolation and fibronectin adhesion assay

Intact normal rhesus macaque TMJs were obtained postmortem from the Oregon National Primate Research Center. Both joints were removed *en bloc* from each animal (juvenile $n = 4$, mean age 1.9 years; adult $n = 4$, mean age 5 years) and disinfected by brief submersion in 70 % ethanol. The TMJ was dissected using sterile surgical technique to isolate the AD defined by the thickening of the anterior and posterior bands (Fig. 1). TAC populations were isolated by sequential treatment with pronase (70 U/mL, 1 h at 37 °C, Sigma-Aldrich) and collagenase II (300 U/mL, 3 h at 37 °C, Worthington Biochemical) (Fig. 1). TACs were subjected to a fibronectin (PeproTech) adhesion assay as described previously (Williams *et al.*, 2010). TACs were seeded (2,000 cells/mL) onto fibronectin-coated 6-well plates for 20 min at 37 °C in 1 mL of DMEM/F12 (ThermoFisher). After 20 min, medium and non-adherent cells were removed. Fresh DMEM/F12 containing penicillin (10,000 U/mL)/streptomycin (10,000 mg/mL), 0.1 mmol/L ascorbic acid, 100 mmol/L HEPES, 1 mmol/L sodium pyruvate, 2 mmol/L L-glutamine and 10 % FBS (DMEM/F12+) was added to the remaining adherent cells. Within 18 h of plating, reference circles were drawn on the bottom of the tissue culture plastic around attached cells, viewing using a Leica inverted microscope (Leica Microsystems). Subsequently, the number of cells adhered was counted based on the reference circles. Reference circles were also annotated to indicate the presence of single cells (shown as Clone 1, Clone 2, Clone 3, *etc.* in Fig. 1) for later use to

ensure clonally derived populations were isolated as described below. Colonies were defined as groups of more than 32 cells with defined boundaries derived from a single cell (Williams *et al.*, 2010) and isolated using sterile cloning rings (Sigma-Aldrich) (Fig. 2). Progenitor cell colonies were expanded to 20 population doublings in DMEM/F12+ supplemented with 1 ng/mL TGF-β1 (PeproTech) and 5 ng/mL FGF-2 (PeproTech) to create cell line stocks. Population doublings were calculated up to 60 population doublings using the equation (Cristofalo *et al.*, 1998):

$$n = [\log(\text{final cell count}) - \log(\text{number of cells initially plated})]/0.301$$

ACPs from hyaline cartilage of rhesus macaque knee joints as well as TPCs from Achilles tendons were also isolated using differential cell adhesion. Clones were isolated in triplicate from each biological replicate and pooled for all molecular characterization studies. Human MSCs isolated from iliac crest bone marrow aspirates were isolated and expanded in monolayer culture as previously described (Johnstone *et al.*, 1998; Markway *et al.*, 2015). The Institutional Review Board at Oregon Health & Science University (Portland, OR, USA) approved bone marrow aspirate isolation from 14 consenting donors (9 females, 5 males, 46-74 years old) (IRB00000605).

Cell differentiation

At approximately 20 population doublings, clonally expanded cell lines were lifted from monolayer using TrypLE (Gibco) and centrifuged at 500 ×*g* for 5 min in 50 mL centrifuge tubes. Following TrypLE aspiration, cells were resuspended in respective differentiation media (osteogenic, adipogenic, or chondrogenic) (Fig. 2). For osteogenic differentiation, cells were suspended in commercial osteogenic medium (Gibco) and plated at 5,000 cells/well in 24-well plates and cultured for 21 d (Oikonomopoulos *et al.*, 2015). For adipogenic differentiation, cells were suspended in adipogenic medium (Gibco) and plated at 30,000 cells/well in 24-well plates and cultured for 21 d (Oikonomopoulos *et al.*, 2015). For fibrochondrogenic differentiation, 100,000 cells/well were pelleted into conical bottom 96-well plates and maintained for 14 d in chondrogenic medium (Anderson *et al.*, 2018; Johnstone *et al.*, 1998) (Fig. 2). Medium was replaced every 2-3 d for all three culture types.

Histological analysis

Alizarin red S and oil red O staining were used to determine the extent of mineralization or lipid formation in osteogenic and adipogenic cultures, respectively. Monolayers cultured in osteogenic or adipogenic medium were fixed in 10 % neutral buffered formalin solution for 10 min. Alizarin red S was used to detect calcium deposition. A stock solution (2 % alizarin red S in deionized water at pH 4.2) was applied to cell monolayers and incubated for 5 min. For lipid detection, a stock solution (0.5 % oil red O in isopropanol) was diluted at a ratio of 2:3 with dH_2O and applied to cells for 1 h. Chondrogenic

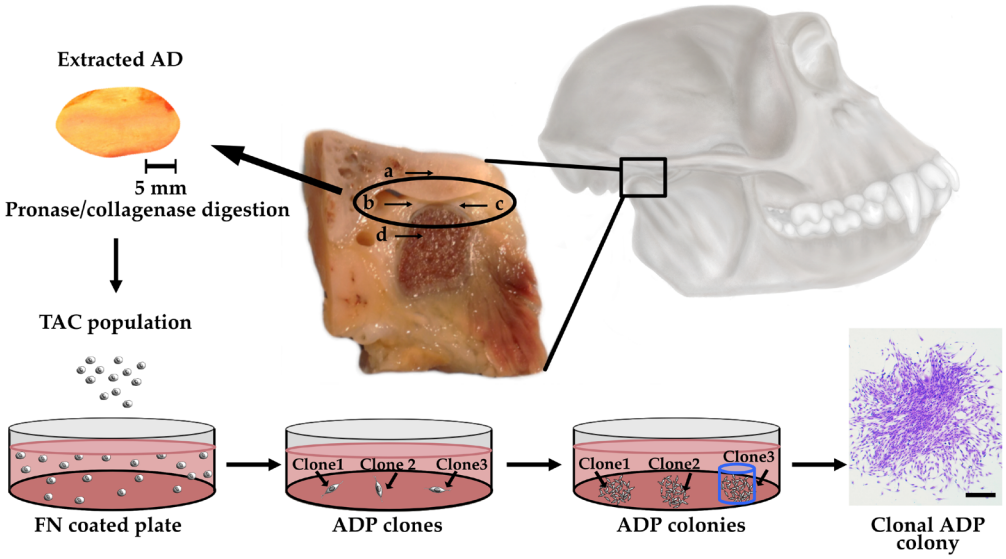

Fig. 1. ADP isolation by differential cell adhesion assay. An *en bloc* rhesus macaques TMJ sample (upper right) illustrating key structures of the TMJ. (**a**) The articular eminence is a portion of the cranial floor. (**b**) Anterior and (**c**) posterior bands define boarders of the AD with the thin avascular, aneural intermediate zone residing between these structures. The AD is attached to (**d**) the mandibular condyle. (**b**,**c**) The AD was extracted intact from these *en bloc* samples. Extracted ADs were digested using pronase and collagenase to obtain the TAC population. TACs were subjected to differential cell adhesion for 20 min on fibronectin-coated plates. The position of adherent cells was marked within 18 h of plating to identify single-cell clones. Clones were numbered to identify colonies derived from single cells, then isolated using cloning rings (blue cylinder) and expanded. Histology image shows an ADP colony derived from a single cell (identified as ADP Clone 3) stained using crystal violet (scale bar: 1,000 μm).

pellets and native macaque ADs were fixed overnight at 4 °C in 4 % paraformaldehyde, embedded in paraffin wax and sectioned for histological analysis (toluidine blue) and IHC (Anderson *et al.*, 2018).

qPCR analysis

At 21 d, monolayers cultured in osteogenic and adipogenic differentiation media were lysed directly from tissue culture plastic using buffer RLT (Qiagen) containing 40 mmol/L DTT. Chondrogenic pellet cultures were lysed using buffer RLT with DTT as previously described (Anderson *et al.*, 2018). RNA was extracted from pellet and monolayer cells using a column-based kit (RNAEasy, Qiagen). Samples (500 ng) were used for reverse transcription to cDNA using qScript cDNA SuperMix (Invitrogen) and diluted (1:10) for qPCR. TaqMan (ThermoFisher) primers (Table 1) were used for qPCR analysis. Cycling parameters and quantitative analysis were performed relative to 18S housekeeping gene, as previously described (Anderson *et al.*, 2018).

Flow cytometry

200,000 cells of rhesus macaque ADPs, ACPs, TPCs, BMMSCs, and TACs were washed twice in PBS containing 1 % BSA by centrifuging at 500 ×*g*, 4 °C, for 5 min. Cells were incubated for 80 min at 4 °C in the dark with antibodies conjugated to CD markers

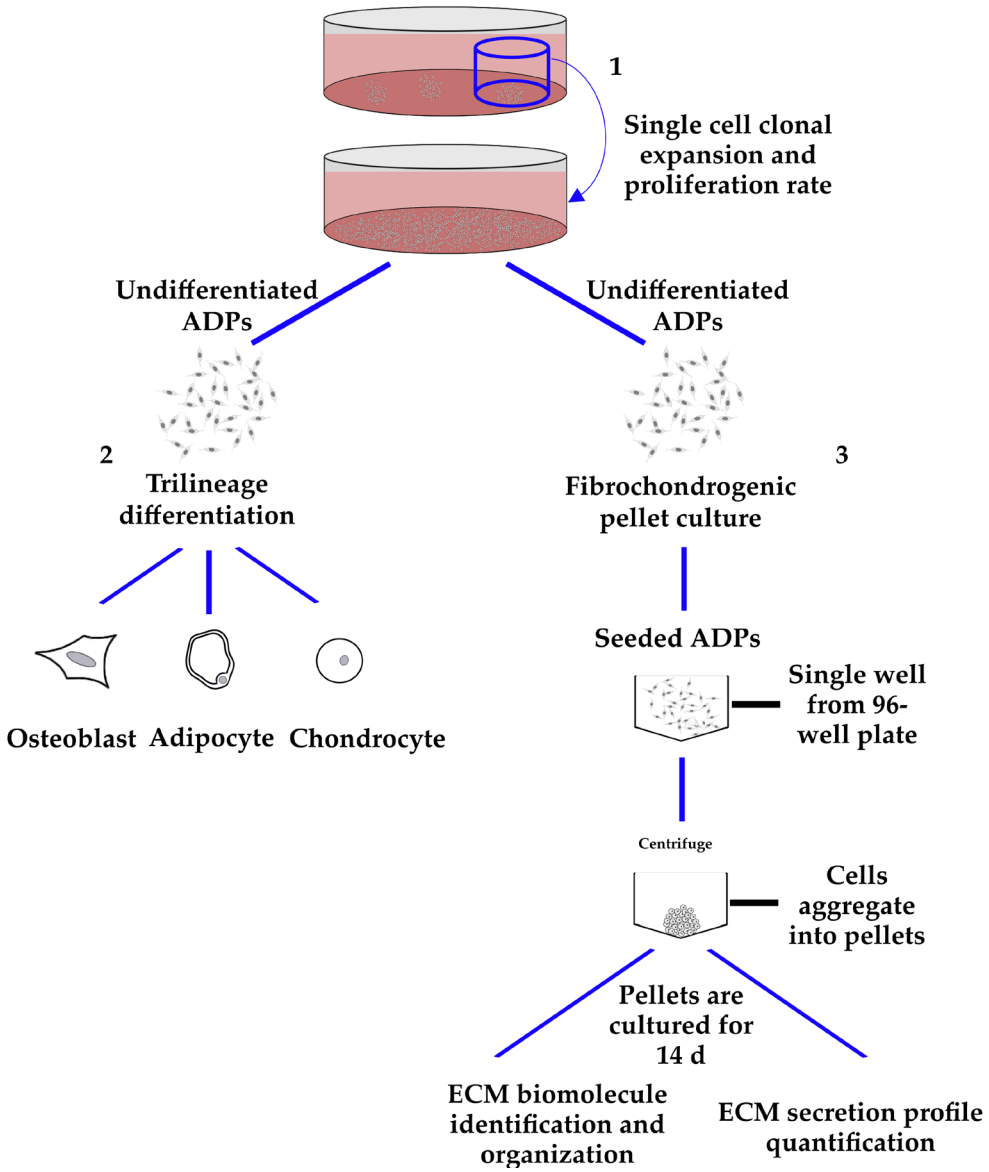

Fig. 2. ADP differentiation experimental design. This diagram outlines the workflow performed on ADPs to determine (1) proliferation rate, (2) stem-cell-like properties and (3) fibrochondrogenic capacity to secrete AD-like ECM molecules. Progenitor cells isolated using differential cell adhesion from the AD, tendon, or cartilage. Chondrogenic differentiation and fibrochondrogenic pellet culture assays were identical. Assay descriptions are altered based on cell source selection due to differing matrix production profiles. Progenitor cells isolated using differential cell adhesion from the articular disc, tendon, or cartilage produced differing ratios of collagen to GAGs, making articular disc and tendon progenitors fibrous, whereas cartilage progenitors favored cartilaginous matrix production with increased GAG and decreased collagen production.

Table 1. qPCR primer information.

Gene	Assay ID	Size (bp)	Annealing temperature (°C)
18S	Hs/Rh99999901_m1	61	60
BGLAP	Rh02890983_m1	96	60
RUNX2	Mf/Rh01047977_m1	59	60
FABP4	Rh02793407_m1	105	60
PPARG	Rh02787679_m1	82	60
SOX9	Rh01001343_m1	101	60
COL1A1	Rh02787848_m1	98	60
COL2A1	Rh01060337_m1	76	60
COL3A1	Rh02787851_m1	86	60
COL6A3	Rh00915111_m1	101	60
VCAN	Rh01007936_m1	95	60

Table 2. IHC and FACS antibody information.

Antigen	Source	Dilution	Company/giftor
Collagen type I	Mouse	1:200	Anthony Hollander, University of Bristol, UK
Collagen type II (II-II6B3)	Mouse	1:200	Developmental Studies Hybridoma Bank, Iowa City IA, USA
Collagen type III (ab7778)	Rabbit	1:200	Abcam
Collagen type VI	Rabbit	1:200	Santa Cruz
Versican	Rabbit	1:200	Abcam
CD105-BV421	Mouse	1:24	Biolegend
CD90-FITC	Mouse	1:24	ThermoFisher
CD34-PE	Mouse	1:24	Becton Dickinson and Company
CD73 PE-Cy7	Mouse	1:24	Becton Dickinson and Company
CD45-APC	Mouse	1:24	Biolegend

(CD105-BV421, CD90-FITC, CD34-PE, CD73 PE-Cy7, and CD45-APC; Table 2) at a concentration of 1 µL per 24 µL of 1 % BSA in PBS, and LD Aqua (ThermoFisher) at 1 µL per 500 µL (25 µL final volume). Cells were centrifuged again at 500 ×*g*, 4 °C, for 5 min, supernatants were removed, and then cells were washed two times in PBS containing 1 % BSA. Next, cells were resuspended in 120 µL fixing solution of 1 % formaldehyde in PBS. Finally, cells were subjected to single-channel FACS analysis using a BD Biosciences-LSR II flow cytometer (Becton, Dickinson and Company). All progenitor cell populations were harvested at 20 population doublings for FACs analysis. BMMSCs and TACs were harvested after first passage for FACS analysis since they are not clonal cell populations.

Biochemical assays

Chondrogenic pellet triplicate samples were rinsed with PBS and digested overnight at 60 °C in 100 µL 4 U/mL papain (Sigma-Aldrich) in PBS containing 6 mmol/L Na_2-ethylenediaminetetraacetic acid and 6 mmol/L L-cysteine pH 6.0. Total sulfated GAG quantification was performed using a DMMB assay (Markway *et al.*, 2013). Collagen secretion was quantified using hydroxyproline as a benchmark by adapting the chloramine-T hydrate oxidation/p-dimethylaminobenzaldehyde method (Markway *et al.*, 2013).

IHC

All paraffin-wax-embedded sections of pellet and native AD tissues were pretreated for antigen retrieval using citrate buffer (pH 6) in a BioWave® equipped with the ColdSpot® system (Ted Pella Inc., Redding, CA, USA), as previously described (Anderson *et al.*, 2018). Then, sections were treated with 1 mg/mL pronase (Roche Diagnostics Corp.) in PBS for 30 min at room temperature followed by 1 mg/mL hyaluronidase in PBS for 30 min at 37 °C. Blocking buffer composed of 5 % BSA was applied for 45 min and, then, sections were probed with the primary antibodies (Table 2). Primary antibodies were diluted in 1 % BSA in PBS, then left on tissue sections overnight at 4 °C. Alexa Fluor 594-conjugated anti-mouse (1:250; Life Technologies) and Alexa Fluor 488-conjugated anti-rabbit (1:200; Life Technologies) secondary antibodies were diluted in 1 % BSA and incubated on the sections for 45 min at room temperature.

For all tissues prepared as negative controls, all steps were performed similarly except for modification to the antibody step. Three experimental negative controls were used, including (1) PBS replacing the primary antibody, (2) tissues incubated with a non-immune antibody of the same species/isotype/concentration, and (3) secondary antibody replaced with PBS. Slides were mounted using ProLong Gold anti-fade reagent containing DAPI

(Life Technologies) and imaged using a Nikon-A1R confocal microscope (Nikon Inc.). Identical image capture parameters and post-image processing settings were used for all compared images.

Statistics

All statistical tests were performed using GraphPad Prism (GraphPad). Experimental design included a minimum of 4 biological replicates (n = 4) and 3 technical replicates for each analytical method. Trilineage mRNA fold change analysis was assessed using a paired t-test to compare changes in mRNA expression over baseline defined as day 0 gene expression prior to differentiation. Unpaired t-tests were performed for all other statistical comparisons. Significance was set at $p < 0.05$ for all statistical tests. Column statistics were used to describe the range and distribution of box and whisker plots.

Results

ADP isolation using differential cell adhesion

Between 5 and 10 discrete colonies were isolated using cloning rings from each biological replicate (Fig. 1). Spindle-shaped fibroblast cell morphology was consistent in all juvenile and adult clonal populations and persisted throughout all population doublings. Juvenile ADPs exhibited a mean CFE of 1.9 % (range of 1-3 %) of the total seeded cell population, while adult samples had a mean CFE of 0.9 % (range of 0.5-1 %) (Fig. 3**a**). By 105 d, all juvenile clones achieved 45 population doublings or more (Fig. 3**b**). One clone from each biological replicate was expanded to assess population doubling rates (Fig. 3**b**). The juvenile cell clones' daily proliferation rate was 0.4582 ± 0.02 population doublings, which was significantly faster than the adult clones' rate of 0.2214 ± 0.05 population doublings ($p < 0.0232$).

ADP clones exhibited heterogeneous matrix production

GAG production was assessed in pellet cultures of 21 adult and 28 juvenile clones from 4 biological replicates each. Chondrogenic pellets from juvenile clones produced more matrix, measured by total GAG and total collagen content (Fig. 4**a**,**b**), compared with pellets from adult clones. Juvenile clones exhibited a wider range of matrix production as measured by total GAG (1 μg to 12 μg) and total collagen (2 μg to 14 μg) compared to adult clones, ranging from 0.5 μg to 6 μg total GAG and 1 μg to 4 μg total collagen (Fig. 4**a**,**b**). Some clones secreted less matrix than the TAC population, while others exhibited superior matrix production compared with TACs (Fig. 4**c**,**d**). Furthermore, clones originating from the same ADP clone that had the largest GAG secretion did not consistently produce the largest amount of total collagen (Fig. 4**c**,**d**). The matrix secretion profile heterogeneity of ADP clones distinguished clonal cell lines that favored fibrous matrix secretion (more total collagen) from those that favored chondrogenic matrix secretion (more total GAG), consistent with known cell type heterogeneity found within the AD (Detamore *et al.*, 2006).

ADPs differentiated into three distinct mesenchymal lineages

Juvenile clones were tested for phenotypic plasticity using osteogenic, adipogenic, and chondrogenic differentiation assays at approximately 20 population doublings. Clones were selected in triplicate from 4 biological replicates. Data were pooled from each biological replicate for all molecular characterization studies. After 21 d, ADP osteogenic cultures formed large nodules of calcium deposits, as marked by increased alizarin red S staining, and showed significantly increased expression of the osteogenic lineage mRNA markers *BGLAP* and *RUNX2* relative to untreated controls (Fig. 5**a**). Similarly, after 21 d, ADP adipogenic cultures exhibited a change in cell morphology from fibroblastic to cobblestoned appearance and showed significantly increased expression of the adipogenic lineage mRNA markers *FABP4* and *PPARG* relative to mRNA expression prior to differentiation (Fig. 5**b**). ADP chondrogenic cultures developed metachromatic staining when stained with toluidine blue, indicating

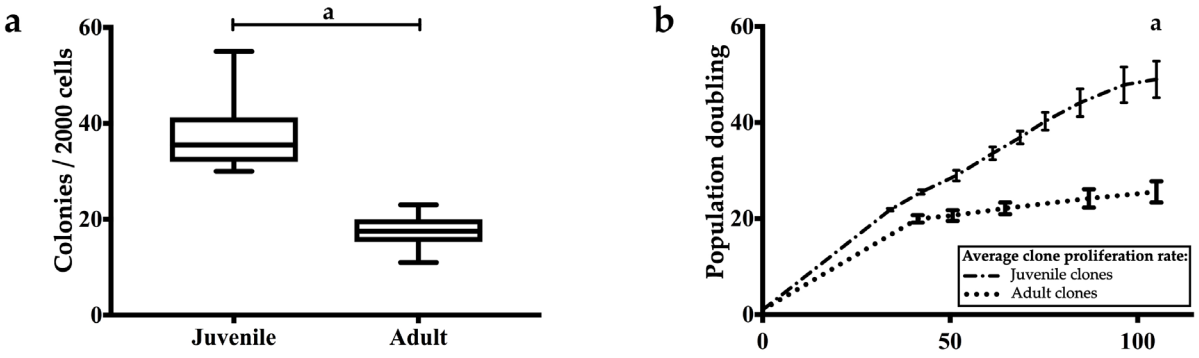

Fig. 3. ADP colony formation and proliferation. (**a**) Colony formation rate of adult ADPs was lower than that of juvenile ADPs ([a]$p < 0.0001$). Box plots illustrate distribution of colony formation. (**b**) The adult ADPs proliferation rate was significantly lower compared with juvenile ADPs ([a]$p < 0.0232$). (**a,b**) Data sets were analyzed using an independent t-test (n = 4).

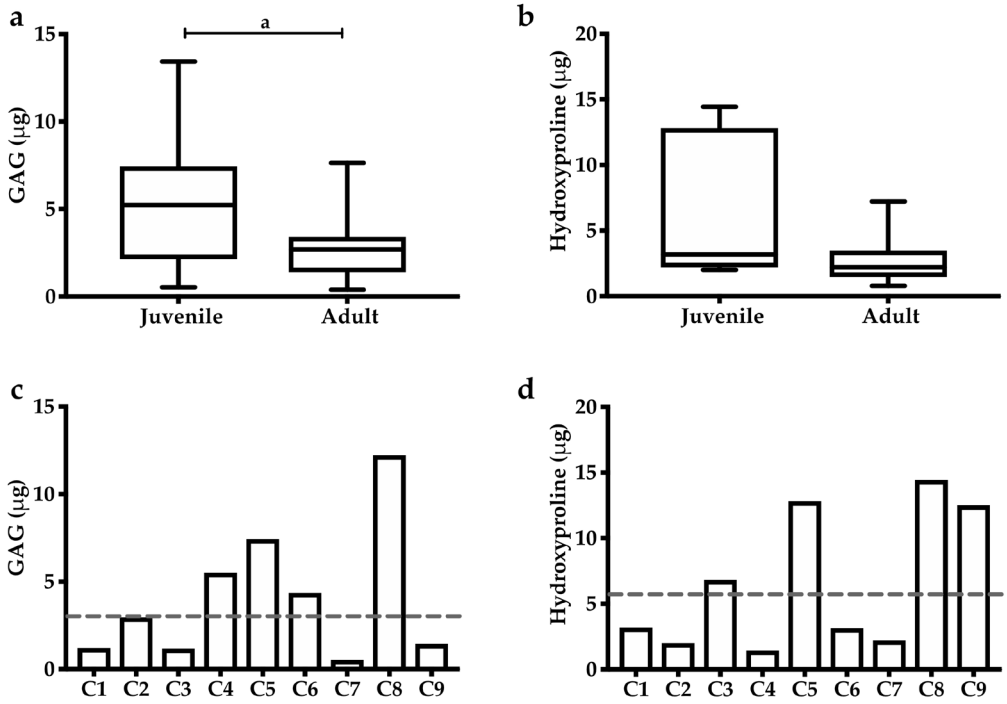

Fig. 4. Juvenile and adult ADPs produced clonally discrete matrix production profiles. (**a**,**b**) Box plots show the average value as well as the maximum and minimum range of total GAG and collagen production. Data sets were analyzed using an independent *t*-test ($n = 4$). (**a**) Juvenile clones produced more GAG than adult clones (independent *t*-test, $^{a}p < 0.0020$, $n = 4$ clones/group). (**b**) Juvenile clones produced more collagen when using hydroxyproline as a reference; however, the difference was not statistically significant (independent *t*-test, $p < 0.0786$). (**c**) GAG clonal heterogeneity from 9 ADP clones of 1 biological replicate. The dashed line indicates GAG secretion of the TACs for the same donor from which the 9 clones were created. (**d**) Clonal heterogeneity also existed with respect to total collagen secretion. (**c**,**d**) Total GAG and collagen were quantified from papain-digested matrices of 9 distinct clonally derived cell lines from 1 biological replicate.

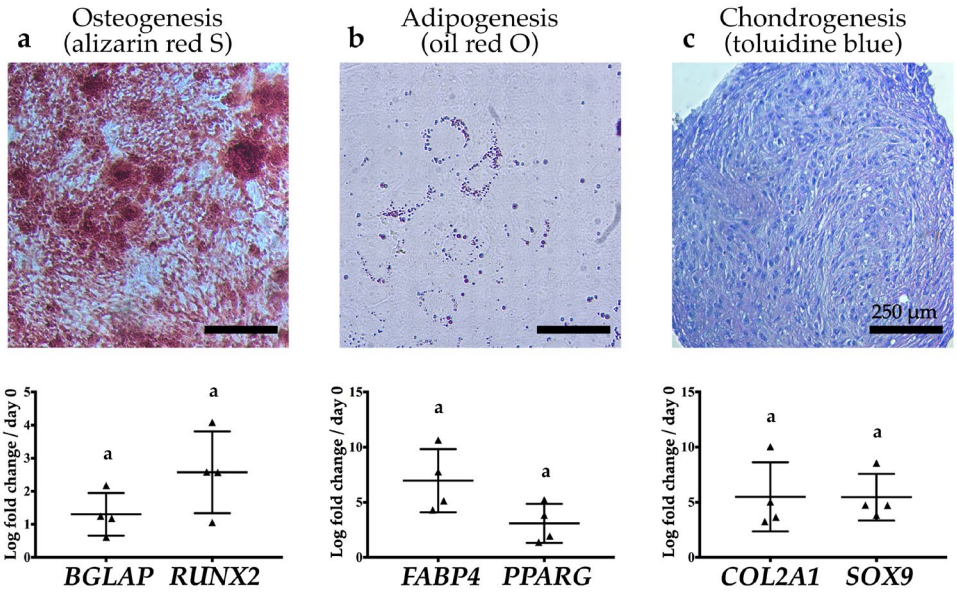

Fig. 5. ADPs differentiated into mesenchymal lineages. (**a**) ADPs deposited calcium (alizarin red S) in their ECM and expressed bone markers *BGLAP* ($^{a}p < 0.0274$) and *RUNX2* ($^{a}p < 0.0250$) when treated with osteogenic supplements in monolayer. (**b**) Differentiated ADPs stored lipids (oil red O) and expressed adipocyte markers *FABP4* ($^{a}p < 0.0166$) and *PPARG* ($^{a}p < 0.0397$) when treated with adipogenic supplements in monolayer. (**c**) In pellet culture with chondrogenic medium, ADPs differentiated into chondrocytes, marked by proteoglycan deposition (toluidine blue), and expressed key chondrocyte markers *COL2A1* ($^{a}p < 0.0349$) and *SOX9* ($^{a}p < 0.0141$). (**a**-**c**) Graphs represent the range of gene expression changes normalized to the 18S housekeeping gene over the baseline (day 0). Paired *t*-tests were utilized to calculate *p*-values for mRNA expression changes over the baseline mRNA expression ($n = 4$ biological replicates) (scale bars: 250 μm).

GAG production. The chondrogenic lineage mRNA markers *SOX9* and *COL2A1* showed significantly increased expression relative to their mRNA expression prior to differentiation (Fig. 5**c**)

FACS analysis of ADPs for putative stem cell CD markers

FACS analysis was used to label ADPs, ACPs, TCPs, BMMSCs, and TACs for a series of positive (CD90, CD73, and CD105) and negative (CD34 and CD45) markers associated with stem cells (Dominici *et al.*, 2006). Analysis of TACs for CD90, CD73, and CD105 revealed a mixture of cell types present in the total cell population, with only a portion of the total cell population positive for these markers (Fig. 6). ADPs showed a similar expression of the positive putative stem cell markers in most of the viable cell population (Fig. 6), consistent with other known progenitor cells (ACPs, TCPs, and BMMSCs). No cell type analyzed in the present study expressed the negative putative stem cell markers CD34 and CD45, which are primarily expected to be found on hematopoietic lineage cells (Dominici *et al.*, 2006).

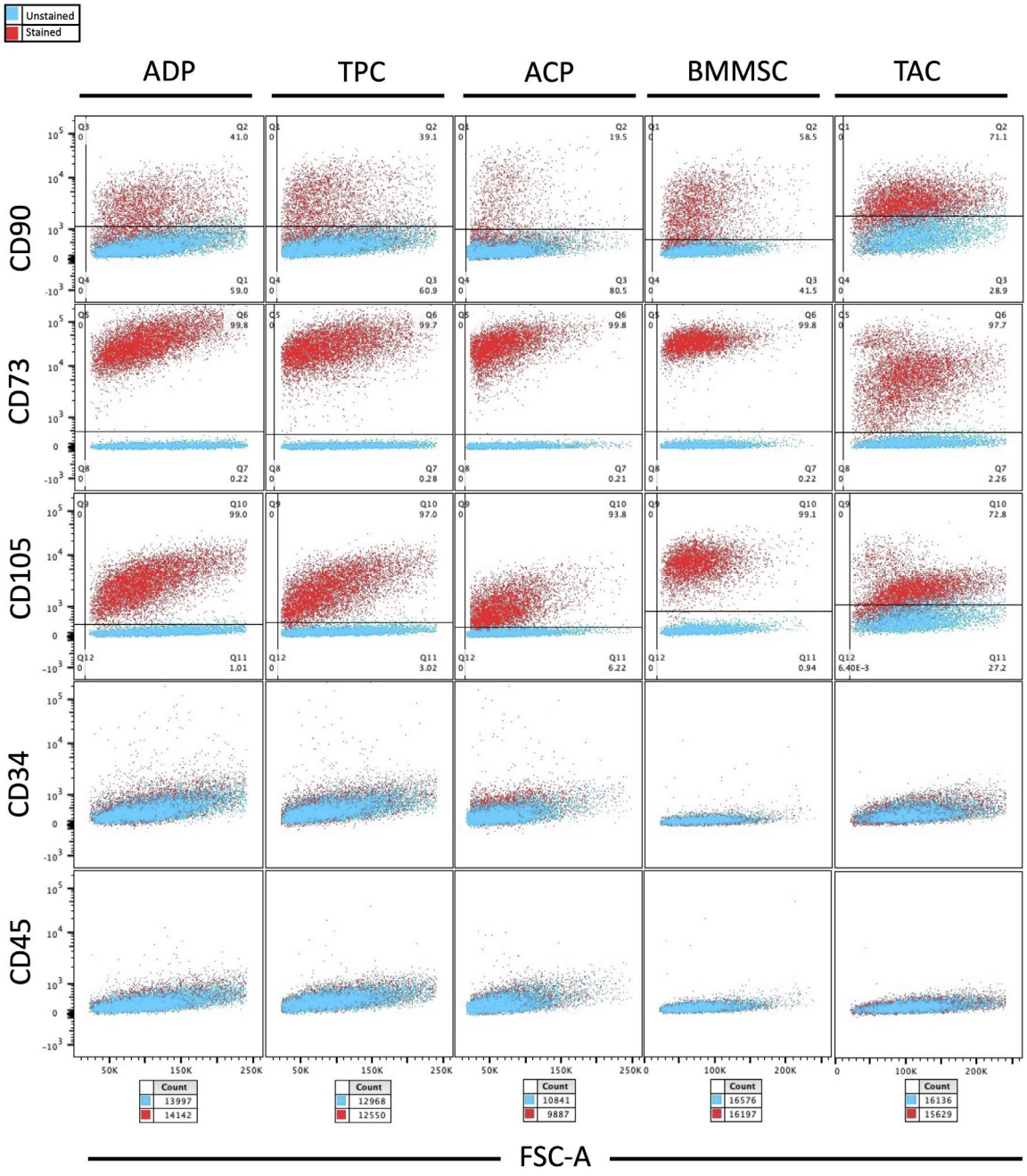

Fig. 6. FACS analysis of putative stem cell markers expressed by ADPs compared to known progenitor cells. ADPs, TCPs, ACPs, BMMSCs, and TACs were analyzed for a series of positive (CD90, CD73, and CD105) and negative (CD34, and CD45) putative stem cell markers. ADPs were compared to known progenitor cells (ACPs, TPCs, BMMSCs) and TACs for positive (CD90, CD73, CD105) and negative (CD34, CD45) stem cell surface markers. Note that TACs displayed a heterogenous population that included a subpopulation following a similar staining pattern as the stem cells, including ADPs. FSC-A: forward scatter area.

ADPs recapitulated native-disc matrix identity

ADP, TPC, and ACP safranin-O-stained pellets showed that tissue-derived progenitor cells produced an ECM that was similar to their tissue of origin (Fig. 7**a**-**c**). ACPs were stained intensely in red, indicating that a higher density of proteoglycans was secreted in the ECM (Fig. 7**c**). Conversely, ADPs and TPCs did not exhibit red staining, indicating that their ECM was more fibrous (Fig. 7**a**,**b**). These findings were supported by hydroxyproline and GAG quantification data, which represented total collagen and proteoglycan content, respectively (Fig. 7**d**,**e**). ADP and TCP pellets contained more total collagen than ACP pellets. A higher total collagen content compared to GAG for ADPs and TCPs was consistent with the fact that that the AD and tendons from which they were derived are fibrous tissues. IHC and qPCR analysis were performed on ADP clones grown in fibrochondrogenic pellet culture and compared with native AD tissue (Fig. 8**a**-**o**). Pellet cultures derived from cells grown out to 60 population doublings maintained positive staining for COL1, COL2, and COL6 in addition to VCAN (Fig. 8**a**,**b**,**d**,**e**,**j**,**k**,**m**,**n**). Abundant COL1 and VCAN staining was found to be diffuse throughout the matrix of pellet cultures and native AD tissue (Fig. **8a**,**b**,**m**,**n**). Notably, COL2 and COL6 were also diffuse throughout the matrix in ADP-derived pellet cultures in contrast to being localized to specific regions of the native AD (Fig. 8**d**,**e**,**j**,**k**). In native AD tissue, COL2 staining was observed only in the compressed posterior band of the AD (Fig. 8**d**). COL6 was observed in this compressed region, localized to the pericellular matrix, indicating a mature state relative to developing tissues (Fig. 8**i**). qPCR data supported these IHC findings (Fig. 8**f**,**l**). *COL2A1* was minimally expressed in the native AD, similarly to IHC results (Fig. 8**d**,**f**). Conversely, ADP pellets had a much higher *COL2A1* mRNA expression, which corresponded with enhanced antibody labeling (Fig. 8**e**). Conversely, *COL3A6* mRNA was consistently expressed in the native AD and pellet tissues (Fig. 8**i**), with uniform antibody staining in both tissues (Fig. 8**g**,**h**).

Discussion

To the authors knowledge, this was the first study to isolate and characterize the proliferation and differentiation capacities of a progenitor cell type isolated from the AD of the TMJ. Although these capacities have been previously demonstrated in mouse cells transfected with human telomerase reverse transcriptase (Park *et al.*, 2015), the present study showed a technique to isolate endogenous single-cell clones from the AD. ADPs satisfy the criteria of tissue-derived progenitor cells, which are described morphologically as fibroblastic cells with

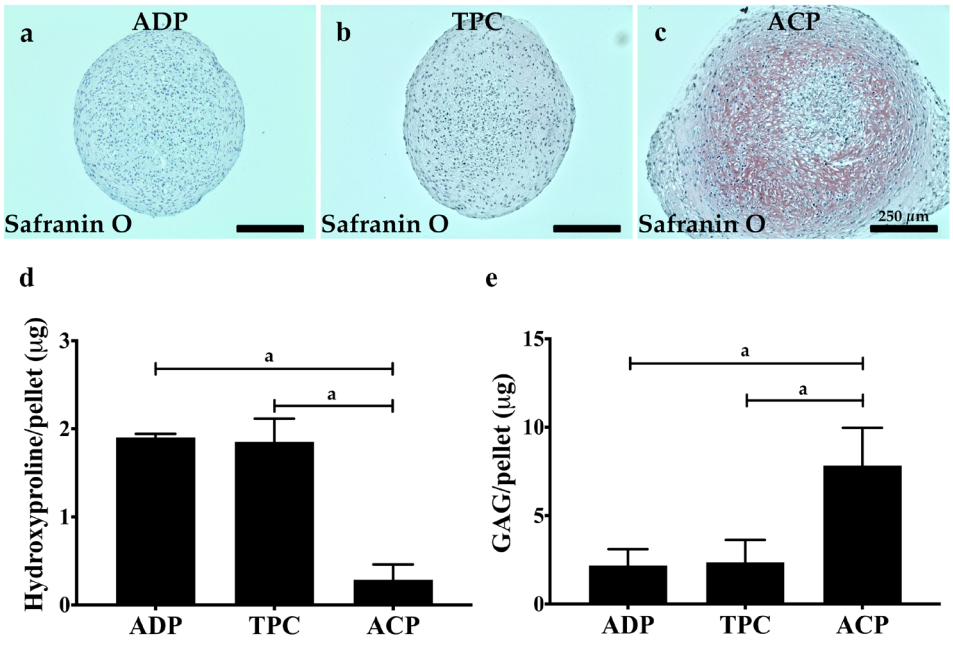

Fig. 7. Progenitor cell matrix secretion was dependent on the tissue of origin. (**a**) ADPs, (**b**) TPCs, and (**c**) ACPs were isolated using differential cell adhesion from the AD, tendon, or cartilage tissues, respectively. (**a**-**c**) Safranin O histology stains illustrated differences in ECM production between ADP, TPC, and ACP after 14 d of chondrogenic differentiation. (**d**) ADPs ($^{a}p < 0.0058$) and TPCs ($^{a}p < 0.0029$) produced more fibrous matrix, indicated by higher total collagen content than ACPs. (**e**) ACPs favored cartilaginous matrix production with increased GAG compared with ADPs ($^{a}p < 0.0419$) and TPCs ($^{a}p < 0.0215$). (**d**,**e**) Data sets presented show the mean with standard deviation of clonal triplicates from each biological replicate. Groups were analyzed using an independent *t*-test ($n = 3$). Data sets were analyzed using an independent *t*-test ($n = 4$) (scale bars: 250 μm).

the potential for self-renewal and differentiation into osteocyte, adipocyte, and chondrocyte mesenchymal lineages (Chen *et al.*, 2018; Mabuchi and Matsuzaki, 2016). The differential cell adhesion technique was utilized to isolate clonal progenitor cells, a method that has been used successfully for isolating clonal progenitor cells from other skeletal tissues (Dowthwaite *et al.*, 2004; Jones and Watt, 1993; Williams *et al.*, 2010; Williamson *et al.*, 2015). ADPs possessed extensive proliferation capacity while maintaining gene and native protein expression, as observed in the AD. The data suggested that ADPs may be a valuable substrate for tissue engineering and regenerative therapies.

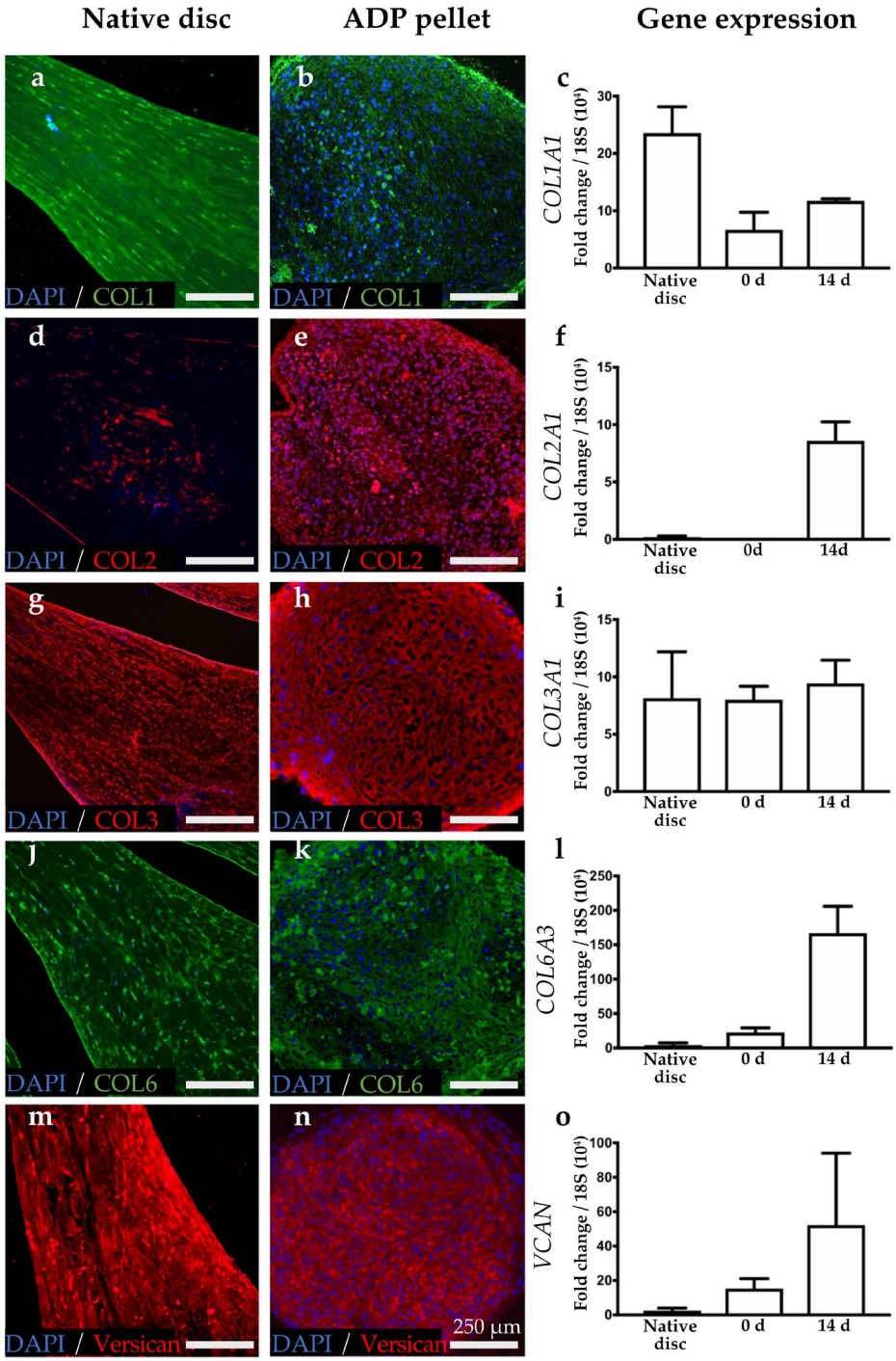

Fig. 8. ADP pellet cultures produced native disc-matrix molecules following clonal expansion. Organization of matrix in the native TMJ AD (left column) was compared with the ADP pellets organization (middle column). Expression of these matrix proteins is also illustrated using qPCR analysis, showing average fold change gene expression with standard deviation (right column) for the native TMJ AD, ADP baseline (0 d), and ADPs following 14 d of pellet culture. (**a**) Native disc COL1, (**b**) ADP pellet COL1, (**c**) qPCR *COL1A1*, (**d**) native disc COL2, (**e**) ADP COL2, (**f**) qPCR *COL2A1*, (**g**) native disc COL3, (**h**) ADP pellet COL3, (**i**) qPCR *COL3A1*, (**j**) native disc COL6, (**k**) ADP pellet COL6, (**l**) qPCR *COL6A3*, (**m**) native disc VCAN, (**n**) ADP pellet VCAN, (**o**) qPCR *VCAN* ($n = 4$ for all IHC and qPCR assays) (scale bars: 250 µm).

ADPs isolated from the TMJ AD demonstrated excellent proliferation potential from single cells, with clones from juvenile animals proliferating beyond 50 population doublings during the observed expansion period. The rate of proliferation also appeared constant through more than 100 *d* in expansion medium, suggesting that the cells retained the ability to continue proliferating beyond the population doubling data shown in Fig. 3**b**. Adult cells proliferated more slowly and it was not clear whether they had the same expansion potential of juvenile cells, as suggested by other studies on articular cartilage progenitors (Williams, 2010). Clonal proliferation would yield billions of cells from a single cell, making ADPs a highly useful cell source for tissue engineering and regenerative medicine applications since they are capable of differentiation and matrix production following significant single-cell expansion. This argument is further strengthened by the clones' continued expression of endogenous AD biomolecules, favoring fibrocartilage matrices with a composition similar to the AD.

Both juvenile and adult ADPs satisfy the basic progenitor cell criteria (self-renewal and multipotent plasticity); however, the juvenile clones are more abundant, proliferate faster, and produce more ECM when compared with adult clones. The age-related differences in ADP self-renewal and differentiation capacity are consistent with those observed for other tissue-specific progenitor cells (Cristofalo *et al.*, 1998). However, the range of variation in adult ADPs indicated that clones exhibiting similar proliferation and matrix-secretion characteristics to juvenile clones persisted in the adult tissue. While ADPs from adult tissues represented a lower percentage of cells isolated, their persistence suggested the possibility of isolating an autologous cell source from adult ADs for regeneration. Importantly, clonal variability further enhanced the utility of isolating ADPs as an autologous cell source since adult ADPs could be screened for a variety of attributes to identify suitable clones for the desired application, including proliferation, matrix secretion, or specific gene profiles of these clonal cell lines.

Once ADPs were defined as a highly expandable clonal progenitor cell type including putative stem cell markers, the study sought to investigate their potential as a cell type for tissue engineering applications. Recently, Anderson and Johnstone (2017) have produced an *in vitro* hyaline cartilage tissue engineering system. Findings indicated increasing total GAG content improved compressive mechanical properties in both the equilibrium modulus and dynamic modulus of the constructs (Anderson and Johnstone, 2017). These findings are consistent with studies concerning the TMJ AD that demonstrated depleting GAG content decreases the compressive mechanical properties of native tissues (Willard *et al.*, 2012). Other studies concerning tensile mechanical properties of fibrocartilage tissues also indicated that improved collagen synthesis enhances the ultimate tensile strength in tissue engineered constructs (MacBarb *et al.*, 2013). Tissue engineering ADs using *in vitro* fibrochondrogenesis techniques has produced advancements in defining cell properties, such as GAG and collagen secretion, that facilitate recapitulating biochemical and mechanical properties inherent to native AD tissue (Detamore *et al.*, 2006; Johns *et al.*, 2008; Kalpakci *et al.*, 2010; Murphy *et al.*, 2013). Prior studies have noted that the TAC population has low GAG production in the fibrochondrogenic assay (Johns *et al.*, 2008). When screening AD cells, it was noted the TAC population had lower matrix secretion, as measured by total GAG, and protein production than some individual clones (data not shown). Thus, an advantage of using ADP clones is the opportunity to select those with specific matrix production qualities for the desired application. This method of assessing suitable cell clones is tunable by choosing optimal clones for different areas of the AD (Detamore *et al.*, 2006). For example, highly GAG secretory clones, which outperform the total TAC population (Fig. 4**c**) would perhaps be suited to engineer the more cartilaginous regions of an AD, while clones secreting more total collagen (Fig. 4**d**) may be suitable for 'sinew-like' regions in the anterior band. Although the pellet culture method utilized in these studies is not suitable for mechanical testing, future directions of this work could focus on applying ADPs into large tissue engineering constructs. These studies would select ADPs based on differential matrix expression for application in larger tissue culture systems to assess differences in tensile and compressive mechanical properties (Anderson and Johnstone, 2017).

Conclusion

The study findings suggested a progenitor cell population was present in the juvenile and adult TMJ AD that bears stem-cell-like properties. This highly expandable cell population exhibited self-renewal and differentiation properties. Single cell, clonal expansion of ADPs to more than 60 population doublings generated millions of cells that maintained important AD biomolecule production characteristics. Distinct clonal ECM production profiles offered flexible selection of matrix secretion profiles to optimize desired outcomes in each assay or treatment application. Importantly, ADPs in the present study represented a robust cell source for AD progenitor cell biology investigations and cell-based regenerative medicine treatment strategies.

Acknowledgements

Thanks to Doctors Deirdre Anderson, Brandon Markway, and John V. Brigande for advice and editing suggestions. Kenneth J. Weekes is a recipient of a National Institute of Dental and Craniofacial

Research NRSA F30 studentship. There are no conflicts of interest associated with this study.

References

Anderson DE, Johnstone B (2017) Dynamic mechanical compression of chondrocytes for tissue engineering: a critical review. Frontiers Bioeng Biotechnology **5**: 76. DOI: 10.3389/fbioe.2017.00076.

Anderson DE, Markway BD, Bond D, McCarthy HE, Johnstone B (2016) Responses to altered oxygen tension are distinct between human stem cells of high and low chondrogenic capacity. Stem Cell Res Ther **7**: 154. DOI: 10.1186/s13287-016-0419-8.

Anderson DE, Markway BD, Weekes KJ, McCarthy HE, Johnstone B (2018) Physioxia promotes the articular chondrocyte-like phenotype in human chondroprogenitor-derived self-organized tissue. Tissue Eng Pt A **24**: 264-274.

Chen KG, Johnson KR, McKay RDG, Robey PG (2018) Concise review: conceptualizing paralogous stem-cell niches and unfolding bone marrow progenitor cell identities. Stem Cells **36**: 11-21.

Cristofalo VJ, Allen RG, Pignolo RJ, Martin BG, Beck JC (1998) Relationship between donor age and the replicative lifespan of human cells in culture: a reevaluation. Proc National Acad Sci U S A **95**: 10614-10619.

Detamore MS, Hegde JN, Wagle RR, Almarza AJ, Montufar-Solis D, Duke PJ, Athanasiou KA (2006) Cell type and distribution in the porcine temporomandibular joint disc. J Oral Maxil Surg **64**: 243-248.

Dominici M, Blanc KL, Mueller I, Slaper-Cortenbach I, Marini FC, Krause DS, Deans RJ, Keating A, Prockop DJ, Horwitz EM (2006) Minimal criteria for defining multipotent mesenchymal stromal cells. The International Society for Cellular Therapy position statement. Cytotherapy **8**: 315-317.

Dowthwaite GP, Bishop JC, Redman SN, Khan IM, Rooney P, Evans DJR, Haughton L, Bayram Z, Boyer S, Thomson B, Wolfe MS, Archer CW (2004) The surface of articular cartilage contains a progenitor cell population. J Cell Sci **117**: 889-897.

Johns DE, Wong ME, Athanasiou KA (2008) Clinically relevant cell sources for TMJ disc engineering. J Dent Res **87**: 548-552.

Johnstone B, Hering TM, Caplan AI, Goldberg VM, Yoo JU (1998) *In vitro* chondrogenesis of bone marrow-derived mesenchymal progenitor cells. Exp Cell Res **238**: 265-272.

Jones PH, Watt FM (1993) Separation of human epidermal stem cells from transit amplifying cells on the basis of differences in integrin function and expression. Cell **73**: 713-724.

Kalpakci KN, Willard VP, Wong ME, Athanasiou KA (2010) An interspecies comparison of the temporomandibular joint disc. J Dent Res **90**: 193-198.

Mabuchi Y, Matsuzaki Y (2016) Prospective isolation of resident adult human mesenchymal stem cell population from multiple organs. Int J Hematol **103**: 138-144.

MacBarb RF, Chen AL, Hu JC, Athanasiou KA (2013) Engineering functional anisotropy in fibrocartilage neotissues. Biomaterials **34**: 9980-9989.

Markway BD, Cho H, Anderson DE, Zilberman-Rudenko J, Holden P, McAlinden A, Otero M, Goldring MB, Johnstone B (2015) Hypoxia-inducible factor 3-alpha expression (HIF-3α) is associated with the stable chondrocyte phenotype and inhibits HIF-2α/ARNTL-mediated transactivation of matrix metalloproteinase-13. Osteoarthritis Cartilage **23**: A153-A154.

Markway BD, Cho H, Johnstone B (2013) Hypoxia promotes redifferentiation and suppresses markers of hypertrophy and degeneration in both healthy and osteoarthritic chondrocytes. Arthritis Res Ther **15**: R92-R92.

Mehrotra D (2013) TMJ Bioengineering: a review. J Oral Biol Craniofac Res **3**: 140-145.

Murphy MK, MacBarb RF, Wong ME, Athanasiou KA (2013) Temporomandibular disorders: a review of etiology, clinical management, and tissue engineering strategies. Int J Oral Maxillofac Implants **28**: e393-e414.

Naujoks C, Meyer U, Wiesmann H-P, Jäsche-Meyer J, Hohoff A, Depprich R, Handschel J (2008) Principles of cartilage tissue engineering in TMJ reconstruction. Head Face Med **4**: 3-3.

Oikonomopoulos A, Deen WK van, Manansala A-R, Lacey PN, Tomakili TA, Ziman A, Hommes DW (2015) Optimization of human mesenchymal stem cell manufacturing: the effects of animal/xeno-free media. Sci Rep **5**: 16570. DOI: 10.1038/srep16570.

Park Y, Hosomichi J, Ge C, Xu J, Franceschi R, Kapila S (2015) Immortalization and characterization of mouse temporomandibular joint disc cell clones with capacity for multi-lineage differentiation. Osteoarthritis Cartilage **23**: 1532-1542.

Salash JR, Hossameldin RH, Almarza AJ, Chou JC, McCain JP, Mercuri LG, Wolford LM, Detamore MS (2016) Potential indications for tissue engineering in temporomandibular joint surgery. J Oral Maxil Surg **74**: 705-711.

Schiffman E, Ohrbach R, Truelove E, Look J, Anderson G, Goulet J-P, List T, Svensson P, Gonzalez Y, Lobbezoo F, Michelotti A, Brooks SL, Ceusters W, Drangsholt M, Ettlin D, Gaul C, Goldberg LJ, Haythornthwaite JA, Hollender L, Jensen R, John MT, Laat AD, Leeuw R de, Maixner W, Meulen M van der, Murray GM, Nixdorf DR, Palla S, Petersson A, Pionchon P, Smith B, Visscher CM, Zakrzewska J, Dworkin SF, Research IRCN International association for Dental, Pain OPSIG International Association for the Study of (2014) Diagnostic criteria for temporomandibular disorders (DC/TMD) for clinical and research applications: recommendations of the International RDC/TMD Consortium Network* and

Orofacial Pain Special Interest Group†. J Oral Facial Pain H **28**: 6-27.

Tong AC-K, Tideman H (2001) The microanatomy of the rhesus monkey temporomandibular joint. J Oral Maxil Surg **59**: 46-52.

Willard VP, Kalpakci KN, Reimer AJ, Athanasiou KA (2012) The regional contribution of glycosaminoglycans to temporomandibular joint disc compressive properties. J Biomechanical Eng **134**: 011011. DOI: 10.1115/1.4005763.

Williams R, Khan IM, Richardson K, Nelson L, McCarthy HE, Analbelsi T, Singhrao SK, Dowthwaite GP, Jones RE, Baird DM, Lewis H, Roberts S, Shaw HM, Dudhia J, Fairclough J, Briggs T, Archer CW (2010) Identification and clonal characterisation of a progenitor cell sub-population in normal human articular cartilage. PloS One **5**: e13246. DOI: 10.1371/journal.pone.0013246.

Williamson KA, Lee KJ, Humphreys WJE, Comerford EJV, Clegg PD, Canty-Laird EG (2015) Restricted differentiation potential of progenitor cell populations obtained from the equine superficial digital flexor tendon (SDFT). J Orthopaed Res **33**: 849-858.

Discussion with Reviewers

David Reed: The clonal heterogeneity of the isolated cells has clear translational potential as you indicate in the discussion of the manuscript. Is the clonal heterogeneity typical for this method of isolation, *i.e.*, do you see clonal heterogeneity in the TAC of ACP cells? Or is the clonal heterogeneity specific to the ADP cells?

Authors: Yes, clonal heterogeneity is typical with this isolation, as previously shown (Anderson *et al.*, 2016).

David Reed: Does the clonal heterogeneity increase as a function of passage number? Will sub-culturing a single clone result in further heterogeneity or does the clone remain homogenous?
Authors: The clone phenotype is typically stable between 20 and 40 population doublings, although some clones senesce as they approach 60 population doublings.

Alejandro Almarza: As a future therapy, do you envision an autologous or allogenic cell source?
Authors: It is unclear whether allogenic ADPs would be immunopriviledged and survive implantation. Future studies will include an examination of this aspect. The use of autologous cells would be possible since biopsies of TMJ tissue is a procedure currently done clinically.

Alejandro Almarza: What is the size of the macaques' disc in comparison to humans?
Authors: According to Kalpakci *et al.* (2011, additional reference), the human disc is approximately 2 × 1 cm. This study did not review the rhesus macaque. However, Fig. 1 shows the scale of one adult macaque disc being approximately the same as the human size reported by Kalpakci *et al.* (2010).

Editor's note: The Scientific Editor responsible for this paper was Thimios Mitsiadis.